Scientific Visualization, 2025, volume 17, number 2, pages 97 - 109, DOI: 10.26583/sv.17.2.07

Implementation of the Set-Theoretic Subtraction Operation in Point Calculus

A.A. Bezditnyi[1]

Melitopol State University

[1] ORCID: 0000-0003-0528-9731, bezdytniy@gmail.com

Abstract

This paper presents an approach to modeling solid geometric objects and their interactions using the apparatus of point calculus in the context of Boolean operations. The study explores the implementation of the Boolean subtraction operation for point-based bodies of various configurations. Parametric point equations are proposed for cuts and holes of different shapes, along with the required modeling parameters and their combinations.

Several modeling techniques are introduced, including the creation of holes through parameter adjustments without modifying the original point equations. This enables the construction of thin-walled structures based on point-defined solids. The method of combining surfaces into a unified body via a current point, with consistent parameter coordination, is also discussed. These techniques eliminate the need for intersection computations between surfaces, thereby avoiding issues such as discontinuities and invalid boundaries. The modeling accuracy is directly dependent on the available computational resources and is ensured by increasing the density of points within the solid object.

To visualize the equations obtained in the work, a point-represented geometric model is used, which is defined as an analytically defined ordered set of points in Euclidean space, formed using parametric equations, possessing a controllable internal structure and not requiring explicit topological connections.

Keywords: geometric modeling, set theorists, boolean operations, geometric solid, point calculus, point solid model.

1. Introduction

Set-theoretic (Boolean) operations play a key role in solid geometric modeling and are widely used to construct complex objects by combining simpler shapes. The main Boolean operations include union, intersection, and difference of geometric objects. These operations make it possible to merge two or more shapes into one, find their intersections, or subtract one or several shapes from another. Boolean operations are broadly applied in CAD systems, engineering design, and physical object modeling, and their implementation has been extensively discussed in both domestic [1] and international [2–5] research.

The union operation creates a single object that includes all areas occupied by each of the original objects. From the set-theoretic perspective, it encompasses all points of the first and second objects, as well as those in the overlapping region.

The difference operation subtracts one object from another, leaving only the part of the first object that does not intersect with the second.

The intersection operation produces a new object consisting solely of the region where the two original objects overlap.

The implementation of Boolean operations in computer-aided design (CAD) systems has always involved a number of challenges [6–8], such as: continuous recalculation and trimming of surfaces at the intersection points of objects; adjustment of edge and vertex connectivity to preserve the topological integrity of constructed models; ensuring correct topology to enable further operations on the models; difficulties in analytically describing complex shapes resulting from subtraction or intersection; the need for accurate detection of intersection regions, often requiring substantial computational resources.

Key aspects of Boolean operations in geometric modeling include working with solid representations such as boundary representation (B-rep), constructive solid geometry (CSG), or voxel models. Boolean operations in such systems require precise computation of new boundaries that arise from intersections. Challenges stem from computational complexity, rounding errors, and numerical instability in object representation. For example, in B-rep, Boolean operations significantly affect the object's topology by altering the structure of faces, edges, and vertices: the number of these elements may change, edges and vertices may split or merge, and the creation of valid boundaries and closed surfaces becomes problematic. This can result in incorrect intersections and invalid geometries.

One significant challenge is the reliable execution of Boolean operations on objects with complex or imperfect boundaries. For instance, if object boundaries are not closed or violate B-rep rules, the results may be incorrect. Precision-related issues also arise, especially in cases where objects intersect over small areas or are nearly tangent, which can lead to errors such as loss of geometry or surface artifacts.

Researchers in geometric modeling have proposed various algorithms to improve the accuracy and robustness of Boolean operations. Approaches include procedural and adaptive modeling techniques that reduce errors by more accurately representing and handling intersections. Recent efforts focus on integrating Boolean operations into modern computing environments using GPUs and parallel computing, significantly accelerating performance.

Despite considerable progress, the problem of improving the reliability and efficiency of Boolean operations remains relevant. Current research aims to develop algorithms that work with arbitrarily complex objects and scale effectively for large models used in architecture, mechanical engineering, and medical visualization.

The use of point calculus in modeling Boolean operations on solid objects offers potential solutions to many of these issues or reduces their complexity. For example, concerns related to storing and processing topological information do not apply to models constructed using point calculus [9,10], as all geometric and spatial information is inherently embedded in a single point-based equation.

It should be noted that within the framework of point calculus, studies focused specifically on set-theoretic operations have not yet been conducted.

2. Description of Methods for Constructing Solid Point-Based Models

2.1. Bodies of Revolution

Methods for implementing set-theoretic operations in point calculus are currently under development, and a unified approach has not yet been established. This section considers several classes of solids with various configurations of cutouts and holes.

The simplest to implement in point calculus are bodies of revolution with axial holes. Their construction relies on a geometric scheme in which the current point of the body begins its movement from the axis. To create such solid models, it is sufficient to adjust the bounds of a linear parameter responsible for filling the interior of the body. As an example, consider the cylindrical model discussed in [12]. Its point equation takes the following form:

$$M = (A - C)u\cos\varphi + (B - C)u\sin\varphi + (D - C)v + C.$$

The linear parameter u, defined in the range from 0 to 1, is responsible for filling the internal space of the cylinder with points. If, for instance, it is limited to the range from 0.5 to 1, the resulting model will be a cylinder with an axial hole whose diameter equals half the diameter of the original cylinder (see visualization in Fig. 2a). Notably, no modification of the point equation is required—only the parameter's range needs adjustment. This modeling technique is suitable for all bodies of revolution that require an axial hole shaped similarly to the original body. Consequently, it significantly simplifies the task of constructing channel-like bodies, as discussed in [11], since there is no need to analytically account for the channel wall, thereby simplifying the resulting equation.

If the shape of the hole differs from that of the body, another modeling technique must be applied. It involves generating an equation for the hole's shell and connecting it to the shell of the primary body using the current point. This method is also suitable when the axis of the hole or cutout does not align with the body's axis.

As an example, consider a simple configuration: a conical cutout within a conical body (Fig. 1). We begin by defining the equation for the cutout. Since the construction of a conical body has already been described in [12], we will write the equation for the lateral surface of the conical cutout based on the given geometric scheme:

$$\begin{aligned} & A_1 = A\bar{p}_A + Cp_A, B_1 = B\bar{p}_B + Cp_B, C_1 = C\bar{p}_C + Dp_C \\ & T_1 = [(A_1 - C)\cos\varphi + (B_1 - C)\sin\varphi + C]p + C_1\bar{p} = \\ & = [(A\bar{p}_A + Cp_A - C)\cos\varphi + (B\bar{p}_B + Cp_B - C)\sin\varphi + C]p + (C\bar{p}_C + Dp_C)\bar{p} = \\ & = (A - C)\bar{p}_A p\cos\varphi + (B - C)\bar{p}_B p\sin\varphi + (D - C)p_C\bar{p} + C \end{aligned} \tag{1}$$

where $\varphi -$ is the angular parameter varying from 0 to 2π, and the parameters p_A, p_B and p_C represent the ratios A_1C to AC, B_1C to BC and C_1C to DC. If the first two parameters are equal, the conical cut will be circular.

Next, we define the lateral surface of the main cone:

$$\begin{aligned} & T = [(A - C)\cos\varphi + (B - C)\sin\varphi \\ & +C]p + D\bar{p} = (A - C)p\cos\varphi + \\ & +(B - C)p\sin\varphi + (C - D)p + D. \end{aligned} \tag{2}$$

It is important to emphasize that the equations (1) and (2) must use the same angular and linear parameters. Synchronization of these parameters within the surfaces being joined via the current point ensures a consistent internal point structure and prevents self-intersections.

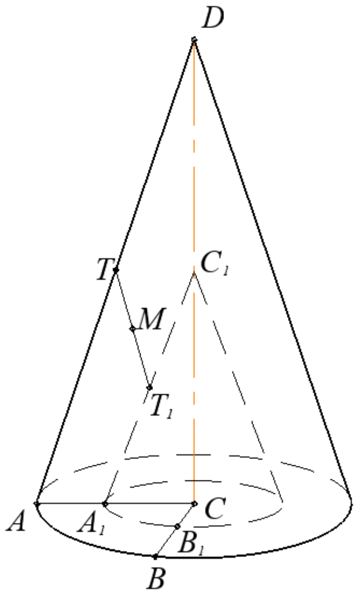

Fig. 1. Geometric diagram of a circular cone with a conical cutout.

We then merge equations (1) and (2) via the current point M, using a linear parameter v, that ranges from 0 to 1:

$$M = T_1 v + T\overline{v} = ((A - C)\overline{p}_A p\cos\varphi + (B - C)\overline{p}_B p\sin\varphi + (D - C)p_C\overline{p} + C)v +$$
$$+((A - C)p\cos\varphi + (B - C)p\sin\varphi + (C - D)p + D)\overline{v} = (A - C)p(\overline{p}_A v + \overline{v})\cos\varphi + \quad (3)$$
$$+(B - C)p(\overline{p}_B v + \overline{v})\sin\varphi + (C - D)(v + p\overline{v} - p_C\overline{p}v) + D.$$

The results of modeling using equation (3) are shown in Fig. 1b. The model consists of 90,000 points. The base radius of the cutout is 75% of the base radius of the main cone, and the parameters p_A and p_B are equal. Additional results with $p_A = 0,5$ and $p_B = 0,75$ are shown in Fig. 1c (for clarity, the model is visualized in cross-section).

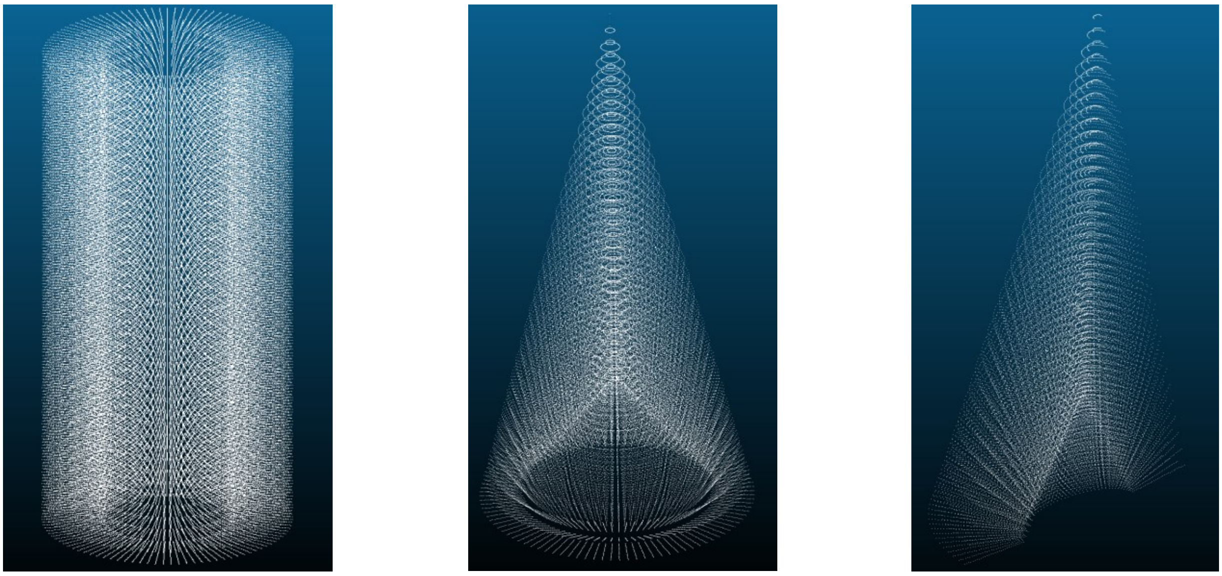

a) b) c)

Fig. 2. Visualization of a cylindrical body with axial hole a), a circular cone with conical cutout b), and a cone with elliptical conical cutout c).

Let us now walk through the modeling of a truncated cone with a vertical elliptical axial hole. The first step is to derive the point equation for the truncated cone (Fig. 3). A similar problem was discussed in [13], although it used a different parameterization, resulting in a different equation.

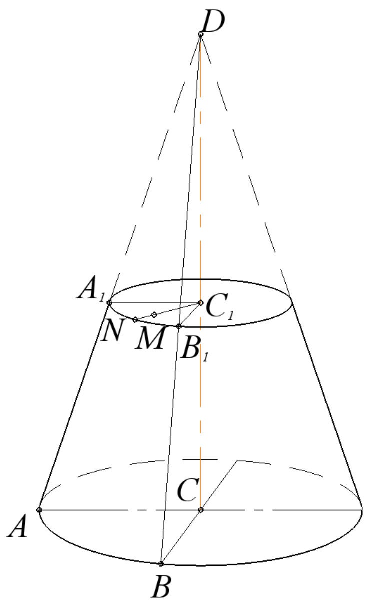

Fig. 3. Geometric diagram of a truncated cone.

We define the current points A_1, B_1, C_1 on segments AD, BD, CD respectively, using a linear parameter $q \in [0,1]$:

$$A_1 = A\overline{q} + Dq; B_1 = B\overline{q} + Dq; C_1 = C\overline{q} + Dq. \tag{4}$$

This defines the vertices of the moving simplex $A_1B_1C_1$, in which the current point of the ellipse N can be determined as:

$$N = (A_1 - C_1)\cos\lambda + (B_1 - C_1)\sin\lambda + C_1, \tag{5}$$

where $\lambda \in [0, 2\pi]$ – is the angular parameter.

The ellipse is then filled with points by using equation (5) to define the current point N:

$$\begin{aligned} N &= C_1\overline{t} + Nt = C_1\overline{t} + [(A_1 - C_1)\cos\lambda + (B_1 - C_1)\sin\lambda + C_1]t = \\ &= C_1\overline{t} + (A_1 - C_1)t\cos\lambda + (B_1 - C_1)t\sin\lambda + C_1t = \\ &= (A_1 - C_1)t\cos\lambda + (B_1 - C_1)t\sin\lambda + C_1 \end{aligned} \tag{6}$$

where $t \in [0,1]$ – is a linear parameter.

We now define the conical body by substituting equations (1) and (3):

$$\begin{aligned} M &= (A\overline{q} + Dq - C\overline{q} - Dq)t\cos\lambda + (B\overline{q} + Dq - C\overline{q} - Dq)t\sin\lambda + \\ &+ C\overline{q} + Dq = (A - C)\overline{q}t\cos\lambda + (B - C)\overline{q}t\sin\lambda + (D - C)q + C. \end{aligned} \tag{7}$$

Equation (7) represents one of the possible formulations for the cone. The parameter q corresponds to height, and the same equation can also be used to model a truncated cone by setting the parameter q range not from 0 to 1, but from 0 to the ratio of the height of the truncated cone to the height of the full cone. It should be noted that for the correct construction of the model it is necessary that the "zero" value of the parameter q defines the lower plane of the cone

Let us complicate the task and model a truncated cone with a vertical axial elliptical hole (Fig. 4).

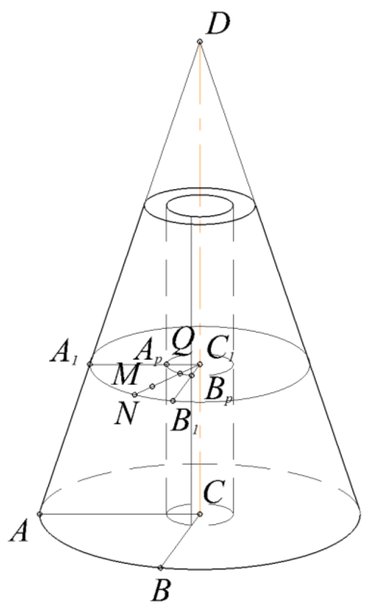

Fig. 4. Geometric diagram of a truncated cone with vertical axial elliptical hole.

The modeling process resembles the previous example, but here the elliptical cutout must be defined by finding points A_p and B_p using the parallel translation formula:

$$A_p = Ap + C\overline{p} + C_1 - C.$$
$$B_p = Bp + C\overline{p} + C_1 - C. \quad (8)$$

where $p = \dfrac{A_pC}{AC}$.

In equations (8), the C_1 point is the current point of the cone axis, which makes it possible to form a moving simplex $A_pB_pC_1$ [14] for constructing a vertical hole. Next, we determine the current point of the elliptical hole with subsequent substitution of (4) and (8):

$$Q = (A_p - C_1)\cos\lambda + (B_p - C_1)\sin\lambda + C_1 =$$
$$= (A - C)p\cos\lambda + (B - C)p\sin\lambda + (D - C)q + C. \quad (9)$$

where $\lambda \in [0, 2\pi]$ – is the angular parameter.

Next, we define point N using (4):

$$N = (A_1 - C_1)\cos\lambda + (B_1 - C_1)\sin\lambda + C_1 =$$
$$= (A - C)\overline{q}\cos\lambda + (B - C)\overline{q}\sin\lambda + (D - C)q + C, \quad (10)$$

We then define the point M on segment NQ using (9) and (10):

$$M = Nt + Q\overline{t} = [(A - C)\overline{q}\cos\lambda + (B - C)\overline{q}\sin\lambda + (D - C)q + C]t +$$
$$+[(A - C)p\cos\lambda + (B - C)p\sin\lambda + (D - C)q + C)]\overline{t} = \quad (11)$$
$$= [(A - C)\cos\lambda + (B - C)\sin\lambda](\overline{q}t + p\overline{t}) + (D - C)q + C,$$

where $t \in [0,1]$ – is a linear parameter.

Equation (11) gives the point-based equation for a truncated cone with an axial elliptical hole (see Fig. 5). For this equation to work correctly, a proper relationship must be established between the fixed parameter p and the maximum value of the variable parameter q:

$$Max(q) = 1 - p.$$

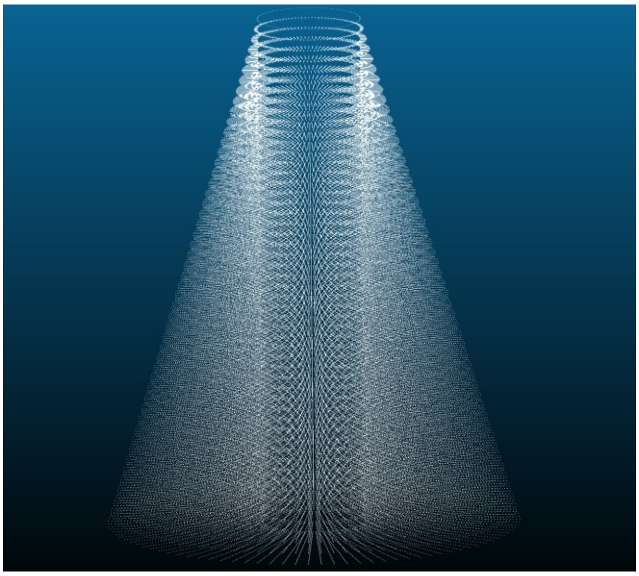

Fig. 5. Point-based model of a truncated cone with axial elliptical hole.

If it is necessary to make a cutout, the shape of which will differ from the shape of the rest of the body, then it is necessary to make changes in the geometric scheme. It is necessary to write an equation of the inner surface of the body and connect it with the outer surface, having previously synchronized their parameters. Synchronization of parameters is an integral part of this method of constructing geometric solid objects, since in the event of a violation of the direction or step of the parameters of the objects being linked together, the geometric properties of the resulting point body will be violated or completely lost.

For example, let us create an analytical description of a spherical body with an elliptical internal cutout (Fig. 6).

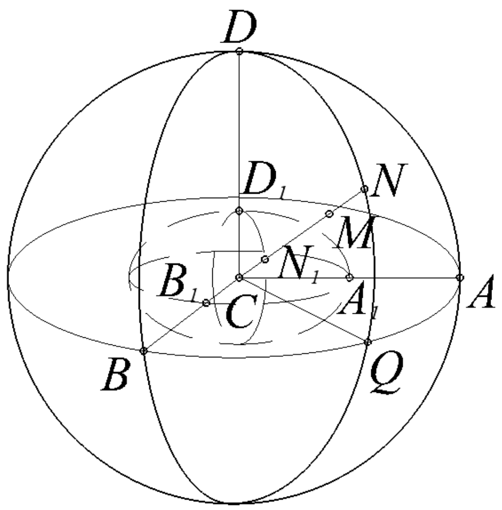

Fig. 6. Geometric diagram of an elliptical body with a cutout

The internal cut is defined by points lying on the axes of the local simplex $ABCD$:

$$A_1 = Ap_A + C\overline{p}_A;$$
$$B_1 = Bp_B + C\overline{p}_B;$$
$$D_1 = Dp_D + C\overline{p}_D.$$

We will take the equation of the elliptic surface from [15]. Moreover, for both the internal and external bodies the equations will be the same, except for the support points. The angular parameters will also coincide, since the points in the bodies must be filled in the same direction and order.

$$N = (A-C)\cos\lambda\cos\varphi + (B-C)\sin\lambda\cos\varphi + (D-C)\sin\varphi + C,$$
$$N_1 = (Ap_A + C\overline{p}_A - C)\cos\lambda\cos\varphi + (Bp_B + C\overline{p}_B - C)\sin\lambda\cos\varphi +$$
$$+(Dp_D + C\overline{p}_D - C)\sin\varphi + C =$$
$$= (A-C)p_A\cos\lambda\cos\varphi + (B-C)p_B\sin\lambda\cos\varphi + (D-C)p_D\sin\varphi + C.$$

where $\lambda \in [0, 2\pi]$ and $\varphi \in [-\frac{\pi}{2}, \frac{\pi}{2}]$.

After obtaining the equations of the shells, it remains to connect them using the current point M by means of a linear parameter $u \in [0;1]$:

$$M = [(A-C)\cos\lambda\cos\varphi + (B-C)\sin\lambda\cos\varphi + (D-C)\sin\varphi + C]\overline{u} +$$
$$+[(A-C)p_A\cos\lambda\cos\varphi + (B-C)p_B\sin\lambda\cos\varphi + (D-C)p_D\sin\varphi + C]u =$$
$$= (A-C)(1-u\overline{p}_A)\cos\lambda\cos\varphi + (B-C)(1-u\overline{p}_B)\sin\lambda\cos\varphi +$$
$$+(D-C)(1-u\overline{p}_D)\sin\varphi + C.$$

The simulation results are presented in Fig. 7.

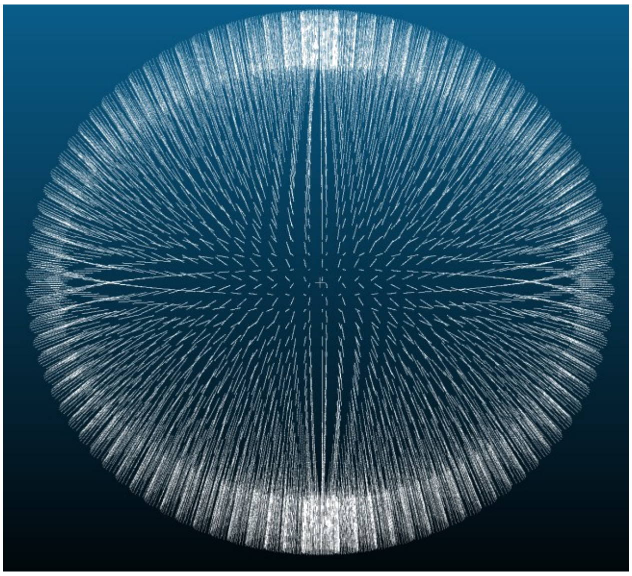

Fig. 7. Point solid model of a sphere with an elliptical inner cutout

The peculiarity of this method of constructing solid geometric objects is the ability to create the internal structure of point bodies of revolution without additional changes in the analytical description, but only by means of working with parameters that determine the internal structure of the body of revolution.

2.2. Polyhedral Bodies

From the standpoint of creating cutouts and holes in point calculus, polyhedral bodies are more complex due to the specifics of their parameterization. This complexity primarily arises because bodies of revolution are usually based on elliptical equations that involve a single angular parameter. Moreover, in the case of rotational solids, it is possible to first generate the surface and only then fill its interior with points using an additional parameter.

The structure of polyhedral bodies in point calculus is fundamentally different. These bodies are formed by linking several straight-line segments using multiple parameters—bypassing the stage of creating a separate surface. As a result, the equation immediately describes a body defined by three parameters. This imposes certain limitations on the configurations of cutouts and holes that can be created in such bodies. The same applies to polyhedral holes or cutouts in bodies of revolution.

As an example, consider the creation of a prismatic axial hole inside a cylindrical body (see Fig. 8).

The equations for cylindrical and prismatic bodies are known from [12]. To construct this configuration, the inner surface of the cutout must be connected to the outer surface via the current point. However, there is a challenge in defining the inner surface: during the construction of prismatic bodies, an explicit equation for their lateral surface is not obtained at any stage.

Nevertheless, it is still possible to extract the point array that represents the lateral surface of a prismatic (or any polyhedral) body. This can be done by generating the full set of body points and then selecting those corresponding to the desired parameter values. The specific parameter values depend on how the body is parameterized. This approach is feasible if a point database is available. However, obtaining an independent analytical description of the full lateral surface–or the complete surface–of a polyhedral body is currently not achievable within the framework of point-based solid modeling.

Therefore, to derive analytical descriptions for various configurations of cutouts in such bodies, it is proposed to divide the body into separate parts during the design phase (based on the number of faces in the body or in the cutout). In the case shown in Fig. 8, this results in four segments.

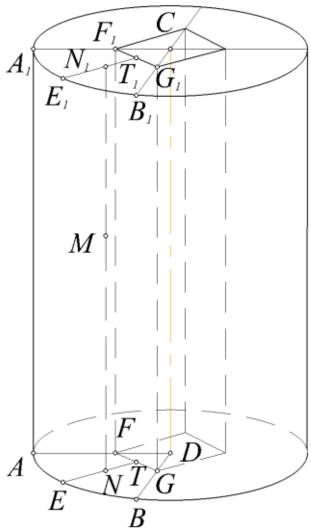

Fig. 8. Geometric diagram of a cylindrical body with a square axial hole

Let us assume a spatial simplex $ABCD$ is given, and on its sides AC and BC – the points F and G are defined, representing the hole's geometry:

$F = Ak + D\bar{k}; G = Bk + D\bar{k}$.

The equation for the lateral surface of the cylinder is written as:

$$E = [(A-D)\cos\lambda + (B-D)\sin\lambda + D]\bar{t} +$$
$$+[(A+C-D-C)\cos\lambda + (B+C-D-C)\sin\lambda + C]t =$$
$$= [(A-D)\cos\lambda + (B-D)\sin\lambda + D]\bar{t} + [(A-D)\cos\lambda + (B-D)\sin\lambda + C]t =$$
$$= (A-D)\bar{t}\cos\lambda + (B-D)\bar{t}\sin\lambda + D\bar{t} + (A-D)t\cos\lambda + (B-D)t\sin\lambda + Ct =$$
$$= (A-D)\cos\lambda + (B-D)\sin\lambda + (C-D)t + D,$$

where $t \in [0;1]$, $\lambda \in [0;2\pi]$.

To generate the body, we link the face of the hole FGG_1F_1 with the corresponding segment of the cylindrical surface using the current point, and coordinate the parameters responsible for forming both the cylinder segment and the wall of the cutout.

We define point T in the straight line and connect it to point E on the arc AB:

$$N = Et + T\bar{t} = [(A-D)\cos\lambda + (B-D)\sin\lambda + D]t + [F(1-\sin\lambda) + G\sin\lambda]\bar{t} =$$
$$= [(A-D)\cos\lambda + (B-D)\sin\lambda + D]t + [(Ak + D\bar{k})(1-\sin\lambda) + (Bk + D\bar{k})\sin\lambda]\bar{t}.$$

This results in a point-filled surface $ABGF$. The parameter $\sin\lambda$ used for the current point T was chosen to synchronize the parameterizations of the arc and the line. Also, $\lambda \in [0; \frac{\pi}{2}]$.

Next, we define the top face of the body $A_1B_1G_1F_1$:

$$N_1 = E_1t + T_1\bar{t} = [(A-D)\cos\lambda + (B-D)\sin\lambda + C]t + [F_1\sin\lambda + G_1(1-\sin\lambda)]\bar{t} =$$
$$= [(A-D)\cos\lambda + (B-D)\sin\lambda + C]t + [([A-D]k + C)(1-\sin\lambda) +$$
$$+([B-D]k + C)\sin\lambda]\bar{t}.$$

Finally, we connect the two obtained points N and N_1 using a parameter v:

$$M = N\bar{v} + N_1v = (A-D)(t\cos\lambda + k\bar{t}(1-\sin\lambda)) + (B-D)(t\sin\lambda + k\bar{t}\sin\lambda) + (C-D)v + D.$$

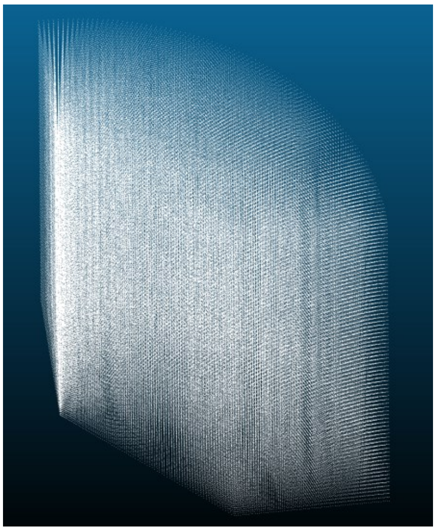

Fig. 9: Point-based model of a circular cylinder segment with a prismatic cutout

To form the complete body, the segment shown in Fig. 9 can be duplicated using a circular array. If the hole is offset, a separate equation must be generated for each segment (the equations will follow the same structure but differ in the constants that define the reference points for the hole).

Now, consider an example of a quadrilateral prism with an elliptical cutout. Let us define a prism in a spatial simplex $ABCD$ with an elliptical hole.

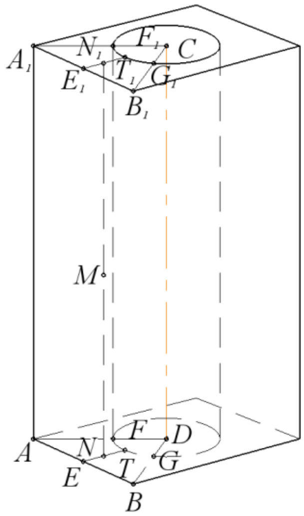

Fig. 10: Geometric diagram of a quadrilateral prism with an elliptical hole

We define the locations of points F and G on lines AD and BD, respectively.

$$F = Ak + D\bar{k};\, G = Bk + D\bar{k}.$$

It should be noted that if the same parameters are used for points F and G, the hole will have a circular shape. If different parameters are applied, the hole becomes elliptical.

Next, we determine the current point N on one plane $ABGF$:

$$N = Et + T\bar{t} = At(1-\sin\lambda) + Bt\sin\lambda + (F-D)\bar{t}\cos\lambda + (G-D)\bar{t}\sin\lambda + D\bar{t} =$$
$$= (B-A)t\sin\lambda + (A-D)(k\bar{t}\cos\lambda + t) + (B-D)k\bar{t}\sin\lambda + D.$$

And then define the current point N_1 on the second plane $A_1B_1G_1F_1$:

$$N_1 = E_1t + T_1\bar{t} = (A+C-D)t(1-\sin\lambda) + (B+C-D)t\sin\lambda +$$
$$+(F_1-C)\bar{t}\cos\lambda + (G_1-C)\bar{t}\sin\lambda + C\bar{t} =$$
$$= (A-D)[t - t\sin\lambda + k\bar{t}\cos\lambda] + (B-D)\sin\lambda[t + k\bar{t}] + C.$$

The final body equation is constructed by connecting points N and N_1:

$$M = N\bar{v} + N_1 v = (B - A)\bar{v}t \sin\lambda + (B - D)\sin\lambda(k\bar{t} + vt) +$$
$$+(A - D)(t - vt\sin\lambda + k\bar{t}\cos\lambda) + (C - D)v + D.$$

All parameters used in these equations are analogous to those described earlier for the cylindrical body with a prismatic cutout. The construction principles and parameter coordination are also the same. An example of visualization is shown in Fig. 11.

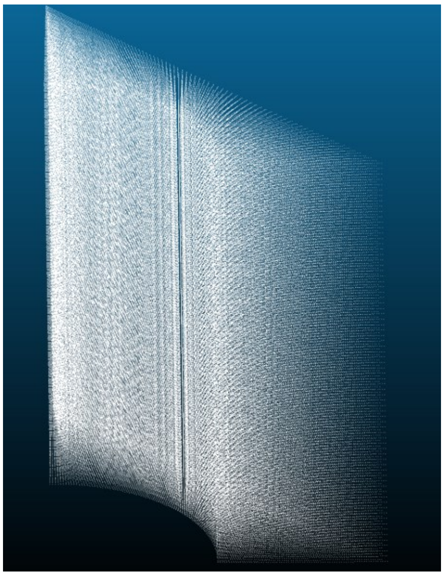

Fig. 11: Point-based segment of a quadrilateral prism with an elliptical hole

To process parametric equations, the author's Point Calculus Software was used (certificate of state registration of the computer program No. 2025610353). The calculation results were exported to .DXF format, after which the resulting arrays of points were visualized using freely distributed software CloudCompare (cloudcompare.org).

3. Conclusion

The conducted study led to the following conclusions:

1. Novel methods for constructing solid models using point calculus have been proposed. Parametric point equations were derived for several types of solids, including rotational and polyhedral bodies with various configurations of holes and cutouts. The resulting models were visualized using a point-based geometric representation.
2. The features of parameterization for the generated models were analyzed, with particular attention to parameter interactions.
3. A method was proposed for creating holes and cutouts in rotational bodies without modifying their equations. The geometric configuration of the model is adjusted through parameter manipulation rather than analytical changes, which significantly reduces the complexity of the model's mathematical description and optimizes computational resource usage.
4. The described modeling techniques allow for flexible geometric modifications without increasing the amount of data required for storage and processing. All resulting models are defined by compact parametric point equations that encode both the external and internal structure of the object, as well as its spatial orientation. These results open the way toward modeling more complex configurations of solid bodies using point calculus.
5. Visualization of the obtained results was carried out using a point-represented geometric model.

References

1. Golovanov N.N. Geometric modeling. DMK Press, 2024. 408 p.
2. C. Hoffmann. Geometric and Solid Modeling. — 2002.
3. R. Rossignac. A.G. Requicha. Solid Modeling // Review article. — 1994.
4. Michael E. Mortenson. Geometric Modeling 2nd Edition. Wiley - 1997.
5. M. Mantyla. An Introduction to Solid Modeling. — 1988.
6. Requicha A.G., Voelcker H.B.. Boolean Operations in Solid Modeling: Boundary Evaluation and Merging Algorithms // Technical Memorandum. — 1984.
7. Arruda M.C.. Boolean Operations on Non-Manifold and B-Rep Solids for Mesh Generation. — 2006.
8. S. Krishnan, M. Gopi, D. Manocha, M. Mine. Interactive Boundary Computation of Boolean Combinations of Sculptured Solids. — 1997.
9. Konopatskiy E.V.. Theoretical Basis of Mathematical Apparatus for Parallel Computing Implementation in Computer-Aided Design Systems / E. Konopatskiy // Programming and Computer Software. – 2024. – Vol. 50, No. 5. – P. 335-342.
10. Konopatsky E.V.. Geometric foundations of parallel computing in computer modeling and computer-aided design systems // Proceedings of the International Conference on Computer Graphics and Vision "Graphicon". – 2022. – No. 32. – P. 816-825.
11. Konopatsky E.V. , Bezditny A.A. The problem of visualizing solid models in the form of a three-parameter set of points (2022). Scientific Visualization 14.2: 49 - 61, DOI: 10.26583/sv.14.2.05.
12. Konopatskiy E.V., Bezditnyi A. A., Lagunova M.V., Naidysh A.V. Principles of solid modeling in point calculus // Journal of Physics: Conference Series: 5, Omsk, March 16–17, 2021. – Omsk, 2021. – P. 012063. – DOI 10.1088/1742-6596/1901/1/012063.
13. Bezditny A.A. Shape-forming operations of extrusion and rotation of solid modeling of geometric objects in point calculus // Bulletin of computer and information technologies. – 2023. – T. 20, No. 1(223). – P. 18-26. – DOI 10.14489/vkit.2023.01.pp.018-026.
14. Malyutina, T. P. Assigning a computer surface of a circle involute by the moving simplex method / T. P. Malyutina, I. P. Davydenko // Bulletin of the Donbass National Academy of Civil Engineering and Architecture. - 2021. - No. 3 (149). - P. 51-55.
15. Konopatskiy E.V., Bezditnyi A.A. Solid modeling of geometric objects in point calculus / CEUR Workshop Proceedings: 31, Nizhny Novgorod, 27–30 sept. 2021. – Nizhny Novgorod, 2021. – P. 666-672.